THE ASTROPHYSICAL JOURNAL, 486:L67–L70, 1997 September 1

SIMULATION OF *f*- AND *p*-MODE INTERACTIONS WITH A STRATIFIED MAGNETIC FIELD CONCENTRATION

P. S. CALLY
Department of Mathematics and Statistics, Monash University, Clayton, Victoria, Australia 3168; paul.cally@sci.monash.edu.au

AND

T. J. BOGDAN
High Altitude Observatory, National Center for Atmospheric Research, Boulder, CO 80307-3000; tom@hao.ucar.edu
Received 1997 May 9; accepted 1997 June 11

ABSTRACT

The interaction of *f*- and *p*-modes with a slab of vertical magnetic field of sunspot strength is simulated numerically in two spatial dimensions. Both *f*-modes and *p*-modes are partially converted to slow magnetoatmospheric gravity (MAG) waves within the magnetic slab because of the strong gravitational stratification of the plasma along the magnetic lines of force. The slow MAG waves propagate away from the conversion layer guided by the magnetic field lines, and the energy they extract from the incident *f*- and *p*-modes results in a reduced amplitude for these modes as they exit from the back side of the slab. In addition, the incident *p*-modes are partially mixed into *f*-modes of comparable frequency, and therefore larger spherical harmonic degree, when they exit the magnetic flux concentration. These findings have important implications for the interpretation of observations of *p*-mode absorption by sunspots, both in terms of the successes and failures of this simple numerical simulation viewed in the sunspot seismology context.

Subject headings: MHD — Sun: magnetic fields — Sun: oscillations — sunspots

1. INTRODUCTION

Thomas, Cram, & Nye (1982) were the first to suggest using observations of sunspot oscillations as a probe of their subsurface structure. Since different *p*-modes sample different depths in the Sun, they reasoned that it should be possible to infer subsurface details such as flux-tube width dependence on depth from observations of umbral Doppler shifts. A complementary approach was developed by Braun, Duvall, & LaBonte (1987, 1988), who observed ingoing and outgoing waves in annuli *outside* of spots. Their unanticipated finding was that sunspots *absorb* up to half of the incident *p*-mode power at favored frequencies and horizontal wavenumbers.

The current observational state of the art is represented by Braun (1995, hereafter B95), who analyzed an uninterrupted time series of 68 hr duration that was obtained in 1988 at the geographic South Pole (Braun et al. 1992). Incoming and outgoing acoustic wave amplitudes and phases were obtained for annular regions around two spots, plage, and quiet-Sun based on measured intensity fluctuations in the core of the Ca II K line. The goal of this effort was to determine accurately the *p*-mode absorption coefficient, α, and scattering phase shift, δ, as a function of the mode parameters. The following instructive observational points emerged from this analysis.

1. Absorption[1] by spots shows no appreciable dependence on azimuthal order m, for $|m| \lesssim 20$, although there is considerable scatter and uncertainty in some of these data.

2. Spots strongly absorb ($\alpha \approx 0.4$) the *f*-mode and *p*-modes for radial orders n of 1 to 6 and for spherical harmonic degrees l up to about 700. Bogdan et al. (1993, hereafter BBLT) find strong absorption in low-order *p*-modes even beyond $l \approx 1000$.

3. Plage absorbs *f*- and *p*-modes less readily than do spots, though with a similar n and l dependence.

4. Spots scatter strongly ($\delta \approx +80°$) with peak values found for axisymmetric ($m = 0$) *p*-modes. There is no discernible scatter from plage.

5. When α is plotted as a function of frequency for a narrow range of spherical harmonic degree l for spots, the results are remarkably similar for *f*- and all *p*-modes independent of n. Most notably, there is a distinct minimum in α between 4.5 and 5.5 mHz. This feature is much less prominent for plage and absent for quiet-Sun.

Any complete theory of *p*-mode absorption must explain these robust properties.

Unfortunately, we are very far from a complete theory at present. Indeed, it would be a great advance if we could settle on the basic physical mechanism. One possibility is that when the *f*- or *p*-modes encounter magnetic field concentrations such as sunspots, there is a partial conversion to magnetoacoustic slow modes, or *s*-modes, and torsional Alfvén waves, which are channeled along the field lines into the solar interior (Roberts & Soward 1983; Spruit 1991; Spruit & Bogdan 1992; Cally & Bogdan 1993; Cally, Bogdan, & Zweibel 1994, hereafter CBZ; Cally 1995; Hindman, Zweibel, & Cally 1996). At large depths, the *s*-modes are essentially Alfvénic in character. It is also likely that the converted waves of sufficiently high frequencies escape *upward* into the overlying atmosphere, again as *s*-modes, though here they are principally acoustic in nature. Idealized numerical eigenvalue calculations, which assume a vertical uniform magnetic field everywhere, suggest that the *f*-mode may be absorbed sufficiently by this process to account for observations but that *direct s*-mode leakage alone probably cannot account for the observed *p*-mode deficits (CBZ). (Simulations presented below suggest, however, that *indirect s*-mode leakage may be occurring, whereby *p*-modes

[1] We use the term "absorption" to indicate a deficit of power emanating from the spot in comparison to that incident on it *in a particular mode*. It may be that some of this is due to conversion into other emergent modes, a process commonly referred to as *mode-mixing*.

first mode-mix into f-modes, which then couple strongly to s-modes.)

In this Letter, we report on a preliminary and rather simplistic numerical simulation designed to improve upon, and to address some inadequacies of, the numerical eigenvalue calculations.

2. MODEL AND SIMULATIONS

We are interested in how an f- or p-mode in a nonmagnetic region couples to magnetoacoustic modes when it encounters an isolated flux concentration. So for simplicity we adopt a Cartesian slab geometry with a vertical, though nonuniform, magnetic field $\boldsymbol{B} = B(x)\hat{\boldsymbol{z}}$. The field $B(x)$ drops continuously to zero at the edge of the slab.[2] Consequently, the magnetic pressure $p_{\rm mag}(x) = B^2(x)/2\mu$ is a continuous function of x alone. The core of the "spot," where B attains its maximum value, is modeled by an adiabatic polytrope of index 1.5 (i.e., $\gamma = 5/3$). Pressure equilibrium then demands that the external pressure be enhanced by a constant, $\max_x\{p_{\rm mag}\}$, over that of the polytrope. The external atmosphere will be called an *enhanced polytrope*. Note that vertical hydrostatic equilibrium ensures that the density is unaffected by this addition. In a realistic atmosphere, the flux slab or tube must flare open with height near the solar surface, modifying this pressure equilibrium.

The maximum magnetic field strength $B_{\rm max}$ is not prescribed directly, nor is it required. Rather, we set the depth L at which the sound and Alfvén speeds coincide. The field strength then follows from $B^2_{\rm max} = 10^6(\gamma - 1)\mu\rho_{00}g(L/10^6)^{5/2}$, where ρ_{00} is the equilibrium density at depth 1 Mm, and all quantities are given in SI units ($g = 274$ m s^{-2}). For concreteness we choose $L = 0.4$ Mm, in the range found by CBZ to yield good results for the f-mode. If $\rho_{00} = 0.01$ kg m^{-3}, say, then $B_{\rm max} = 4820$ G. It should be borne in mind that this is a field strength at the equipartition depth; in a realistic flaring field sunspot model the surface field would be considerably reduced.

The external enhanced polytrope has a temperature profile that is of course linear at depth but that attains a minimum a little below the surface before asymptotically moving upward as $z \rightarrow 0$. With our choice of L, and taking a value of 0.6 for the mean molecular weight, the temperature minimum is 5775 K at $z = -0.44$ Mm; $T = 9054$ K at the top of our computational domain situated at $z = -0.2$ Mm (see Figs. 1 and 2 [Pl. L4] and Figs. 3 and 4 [Pl. L5]). This behavior is qualitatively not unrealistic.

The simulation code is based on a finite difference discretization of the linearized MHD wave equations written in conservation form. A staggered grid is used to ensure strict numerical conservation. Time stepping uses a Lax-Wendroff–type two-step method that yields essentially no numerical diffusion. Since we are dealing with the linearized equations (perfectly adequate here), the well-known shortcomings of Lax-Wendroff schemes for shocks are of no concern. Our simulations use a 1000×120 grid for the f- and p_1-modes and a 1000×200 grid for p_2 and p_3. There is neither any y dependence in the problem, nor any y components of velocity or magnetic field. Therefore, the transverse Alfvén wave is absent from our simulations, and resonance absorption is possible only in the slow continuum (Goedbloed 1983; Goossens, Poedts, & Hermans 1985; Keppens 1996; Beliën, Poedts, & Goedbloed 1996; Cally & Maddison 1997).

In our simulations, we excite an f- or p-mode on the left-hand boundary of our computational box $0 < x < 130$ Mm, $z_{\rm bot} < z < -0.2$ Mm, by imposing the horizontal velocity there based on the exact eigenfunction for the appropriate mode in the nonmagnetic enhanced polytrope in the case in which periodic boundary conditions are applied on the left and right. On the right-hand boundary we apply a projected characteristic outgoing wave boundary condition (Thompson 1987). This is not perfect, since our modal rays do not generally strike the boundary normally, but it provides good performance in most cases, particularly if this right-hand boundary is set far enough away from the region of interest. The projected characteristic boundary condition is also applied at the base, though this is not crucial, as we set $z_{\rm bot}$ deep enough to be well down in the evanescent tail. Specifically, we choose $z_{\rm bot} = -15$ Mm for f and p_1, and -25 Mm for p_2 and p_3, and place a magnetic field concentration between $x = 20$ Mm and $x = 50$ Mm. The total width (30 Mm) is comparable to a sunspot diameter. The field is uniform between 25 and 45 Mm and ramps up to this value continuously from the two edges. The zero of z is where the internal polytropic density and pressure would vanish.

At the top we impose the stress-free conditions $\delta\mathcal{M}_{zz} = 0$ and $\delta\mathcal{M}_{xz} = 0$, where δ signifies the Lagrangian perturbation, and $\mathcal{M}_{ij}$ is the MHD stress tensor. The first yields $c^2\ \mathrm{div}\ \boldsymbol{v} = a^2\partial u/\partial x$, and the second $b_x = 0$, where c is the sound speed, a the Alfvén speed, u the horizontal fluid velocity, $\boldsymbol{v}$ the velocity vector, and b_x the horizontal component of the magnetic field perturbation. In the absence of a magnetic field, the first reduces to the vanishing of the Lagrangian pressure perturbation. These boundary conditions, though ostensibly quite reasonable, are rather arbitrary. A more realistic model should impose some form of overlying atmosphere that reflects waves below the chromospheric acoustic cutoff frequency ($\approx$5–6 mHz) and allows those above it to escape upward.

3. RESULTS

Many insights are to be gained by watching movies of the simulations. However, in this Letter we shall restrict ourselves to presenting several "stills" from such movies in Figures 1–4. Figures 1 and 2 show the interaction of an f-mode and p_2-mode of identical horizontal wavelengths $\lambda = 10$ Mm (corresponding to $l = 437$), with a magnetic flux slab (their respective frequencies are 2.09 mHz and 4.08 mHz). Figures 3 and 4 show the interaction of a p_1-mode and p_3-mode of identical frequencies $\nu = 4.08$ mHz with the same magnetic slab. All figures pertain to a time when the system has essentially settled down to a steady state in response to the imposed mode driving at the left boundary of the computational domain. Viewing the transient behavior does not appear to provide any important new insights, so in the interests of brevity it is not discussed here. The driving eigenfunction is normalized to have unit amplitude in the vertical velocity w at the temperature minimum in the enhanced polytrope. The lower portion of each figure gives a rendering of the x-z behavior of the horizontal velocity $u(x, z, t)$, while the line plots in the top portion of the figures give the square of the vertical velocity $w^2(x, t)$ (*heavy line*) on the dotted isotherm $T = 5775$ K (the temperature minimum in the nonmagnetic region), and a comparison

[2] A numerical instability develops if $B(x)$ is discontinuous. This could be overcome with a purpose-built code in which interfaces are handled without finite differences being taken across them, but there seemed little point to this in the current problem.

$w^2(x, t)$ for a pure p-mode in the absence of a magnetic field[3] (*thin dashed line*).

In these representations of the horizontal velocity field, all four figures exhibit roughly the same basic features. In the unmagnetized regions and in the weakly magnetized ($p_{\rm mag} \ll p_{\rm int} \approx p_{\rm ext}$) lower portion of the magnetic slab, the p-modes and f-mode are distinguished by their alternating lobes of leftward- and rightward-directed horizontal velocities. With the passage of time these lobes move steadily toward the right. In the upper part of the flux slab these alternating horizontal velocity lobes are inclined with respect to the vertical and become nearly horizontal and very tightly packed with increasing depth. These are the signatures of the downward-propagating "Alfvénic" s-modes, and the tighter spacing of the lobes with depth is simply a consequence of the rapid decrease of the Alfvén speed with increasing depth. As they propagate deeper into the magnetized atmosphere, the s-modes become increasingly decoupled from the rightward propagating p-modes and only the independent superposition of these two independent modes results in the modulation of each of their respective patterns that is especially apparent in Figures 1 and 2. The leading edge of the s-mode is generated predominantly in the magnetic boundary layer between $x = 20$ Mm and $x = 25$ Mm. With the passage of time, the downward-propagating s-mode wave front continues to maintain connectivity on its trailing edge with the predominantly acoustic wave with which it shows a strong tendency to be aligned, but it propagates across the strong magnetic field in the $a \approx c$ "Wilson depression" of the flux slab. Numerous thin striations are also visible in the fore and aft magnetic boundary layers that separate the flux slab from its nonmagnetic environment. This fine-scale structure may well be a symptom of phase-mixing associated with the resonance absorption phenomenon, but it nevertheless appears to be carried into the uniform core of the flux slab by the downward propagation of the s-modes. The grid resolution seems to be adequate for the s-modes in each of the figures. The visible striations would also appear to be resolved, although it is possible that the grid is not sufficiently fine to allow the formation of smaller scale structure.

All the incident modes generate downward propagating s-modes in the magnetic flux concentration, and this MHD mode-conversion process ultimately leads to the reduced mode amplitudes found behind the flux slab. This is qualitatively consistent with observational points 1 and 2. In contrast to the eigenvalue calculations of CBZ, which took no account of the interaction between the flux slab and its nonmagnetic surroundings, the time-dependent simulations presented here, if anything, err somewhat on the side of predicting a little too much p-mode absorption. For example, the emerging p_1-mode on the right side of Figure 3 has its energy reduced in magnitude by perhaps 60%–70%. This is well in excess of $\alpha \approx 0.4$ reported by BBLT for the $l \approx 674$ p_1-mode. Such a discrepancy could well be related to the slab geometry providing an overestimate[4] of α coupled with the observations tending to underestimate the true α as a result of the relatively short p-mode lifetimes that obtain at these large spherical harmonic degrees (BBLT). For the f-mode of Figure 1 the inferred absorption coefficient is in excellent agreement with that reported by B95. However, at higher frequencies of 3 mHz ($l \approx 850$) and 4 mHz ($l \approx 1500$) simulations not explicitly shown in this Letter indicate nearly complete conversion of the f-modes to s-modes within the magnetic slab, contrary to observational evidence.

Unlike the incident f-modes, which leave the flux slab (much) reduced in amplitude and advanced in phase, the three incident p-modes all exhibit significant mode-mixing behind the magnetic flux slab, and they emerge with *retarded* phases, in disagreement with observational point 4. In every case (Figures 2, 3, and 4) the f-mode having the smallest allowed wavelength for the prescribed driving frequency is generated by the presence of the magnetic slab and is mixed with the transmitted p-mode. In view of the findings noted above, that f-modes between 3 and 4 mHz are almost totally absorbed by the magnetic slab, this downward conversion (in radial order) of p-modes to the f-mode at a fixed frequency begins to explain why the observations fail to show f-mode absorption coefficients much in excess of 0.5–0.6 in the 5 minute band (BBLT).

A direct comparison of phase shifts between our planar and the actual cylindrical geometries is probably a futile exercise. Rather, we would simply point out that the negative phase shifts experienced by the transmitted p-modes are essentially a consequence of the reduced wavelength of that mode within the magnetic slab relative to its wavelength in the surrounding enhanced polytrope. Consistent with the findings of CBZ, the imposition of a vertical magnetic field upon a polytrope does act to *increase* the horizontal wavelength of a mode at fixed frequency, but the temperature rise of the enhanced polytrope confining the magnetic slab also acts to increase the wavelength for p-modes and is even more effective in this regard than the imposed magnetic field within the slab. As an example, eigenvalue calculations yield the following wavelengths (Mm) for the p_2-modes of frequency 4.089 mHz in an atmosphere truncated at $z = -0.2$ Mm (see Fig. 2): enhanced polytrope (the external atmosphere), 10 Mm; polytrope (the internal atmosphere without the magnetic field), 9.77 Mm; and magnetic polytrope (the internal atmosphere with $L = 0.4$ magnetic field), 9.84 Mm. Thus, although the magnetic field does increase the horizontal wavelength over that in the polytrope, it is still less than that in the external enhanced polytrope, hence our negative phase shifts, contrary to what is actually observed (Abdelatif, Lites, & Thomas 1986). This is obviously an artifact of our unrealistic vertical magnetic field configuration.

Finally, we should mention that the reduced amplitude of $w^2(x)$ within the magnetic slab is entirely due to the temperature-minimum isotherm dipping downward into denser fluid within the magnetic flux slab. If the profile of $w^2(x)$ were to be plotted along an isopycnic (i.e., curve of constant density), then for the incident p-modes, enhanced levels of $w^2(x)$ and reduced levels of $u^2(x)$ would be present within the magnetic slab compared to their characteristic values on the fore side of the flux slab. For the incident f-mode, on the other hand, the contrary is found to apply in better agreement with the observed suppression of 5 minute oscillations within sunspots (Lites et al. 1997) and plage (Brown et al. 1992; Hindman 1997).

4. SUMMARY

The simulations presented here demonstrate convincingly the presence of an efficient MHD mode-conversion process that operates within sunspot-like magnetic flux concentrations.

[3] Again along the $T = 5775$ K isotherm, which in this nonmagnetic case is everywhere at $z = -0.44$ Mm.

[4] For the slab, the modes must pass through its entire width, whereas an encounter with a cylinder may be more or less glancing.

They also lend strong support to the notion that sunspots can mix incoming and outgoing p-modes of comparable frequencies. In fact, Figures 1–4 go a little beyond this overall idea and suggest a preference for a downward conversion from higher to lower radial orders—or equivalently, an upward conversion from small to large spherical harmonic degrees. Because of the highly idealized geometry and equilibrium structure adopted in these preliminary investigations, it comes as no surprise that these simulations fail to provide absorption coefficients and phase shifts that are in good quantitative agreement with the observations. On the other hand, the overall, qualitative similarities between our simulations and the observations are sufficiently compelling to suggest that the simple model captures some—but not all—of the important features of f- and p-mode absorption by sunspots. There are also many points of disagreement, particularly concerning phase shifts and the suppression of 5 minute oscillations within sunspots. Five crucial features that should be introduced in order to begin to rectify these disagreements are cylindrical geometry, divergence of the sunspot magnetic field with height, more realistic transmitting upper boundary conditions (perhaps involving the imposition of a realistic overlying atmosphere), intermittent magnetic fibril structure within the spot, and convective extinction and generation of high-l modes within the computational domain (CBZ).

Work is currently underway with regard to the first two of these five planned improvements to the physical model. The implementation of a diverging magnetic field geometry is particularly promising, as it would appear that if higher radial order modes of frequencies in the range considered here are to be significantly absorbed, then the $a \approx c$ (i.e., plasma $\beta \approx 1$) region must extend to greater depths than are implied by the vertical field model, so as to tap the modes' energy more effectively. Recent inversion efforts based upon a phenomenological absorption parameter also lend support to this notion (Chen et al. 1997). The fragmentation of the sunspot into intermittent magnetic fibrils below the visible solar surface is likely to further enhance the strength of this interaction, since the $\beta \approx 1$ fibrils may be distributed over an area comparable to the visible surface extent of the spot.

P. S. C. wishes to thank the High Altitude Observatory for its hospitality while most of this work was being carried out. A hypergeometric function subroutine used in our calculations was kindly supplied by Brad Hindman. The National Center for Atmospheric Research is sponsored by the National Science Foundation.

REFERENCES

Abdelatif, T. E., Lites, B. W., & Thomas, J. H. 1986, ApJ, 311, 1015
Beliën, A. J. C., Poedts, S., & Goedbloed, J. P. 1996, Phys. Rev. Lett., 76, 567
Bogdan, T. J., Brown, T. M., Lites, B. W., & Thomas, J. H. 1993, ApJ, 406, 723 (BBLT)
Braun, D. C. 1995, ApJ, 451, 859 (B95)
Braun, D. C., Duvall, T. L., & LaBonte, B. J. 1987, ApJ, 319, L27
———. 1988, ApJ, 335, 1015
Braun, D. C., Duvall, T. L., LaBonte, B. J., Jefferies, S. M., Harvey, J. W., & Pomerantz, M. A. 1992, ApJ, 391, L113
Brown, T. M., Bogdan, T. J., Lites, B. W., & Thomas, J. H. 1992, ApJ, 394, L65
Cally, P. S. 1995, ApJ, 451, 372
Cally, P. S., & Bogdan, T. J. 1993, ApJ, 402, 721
Cally, P. S., Bogdan, T. J., & Zweibel, E. G. 1994, ApJ, 437, 505 (CBZ)
Cally, P. S., & Maddison, S. T. 1997, J. Plasma Phys., 57, 591
Chen, H.-R., et al. 1997, ApJ, submitted
Goedbloed, J. P. 1983, Physica, 12D, 107
Goossens, M., Poedts, S., & Hermans, D. 1985, Sol. Phys., 102, 51
Hindman, B. W. 1997, ApJ, in preparation
Hindman, B. W., Zweibel, E. G., & Cally, P. S. 1996, ApJ, 459, 760
Keppens, R. 1996, ApJ, 468, 907
Lites, B. W., Thomas, J. H., Bogdan, T. J., & Cally, P. S. 1997, ApJ, submitted
Roberts, P. H., & Soward, A. M. 1983, MNRAS, 205, 1171
Spruit, H. C. 1991, in Challenges to Theories of the Structure of Moderate Mass Stars, ed. J. Toomre & D. O. Gough (Berlin: Springer), 121
Spruit, H. C., & Bogdan, T. J. 1992, ApJ, 391, L109
Thomas, J. H., Cram, L. E., & Nye, A. H. 1982, Nature, 297, 485
Thompson, K. W. 1987, J. Comp. Phys., 68, 1

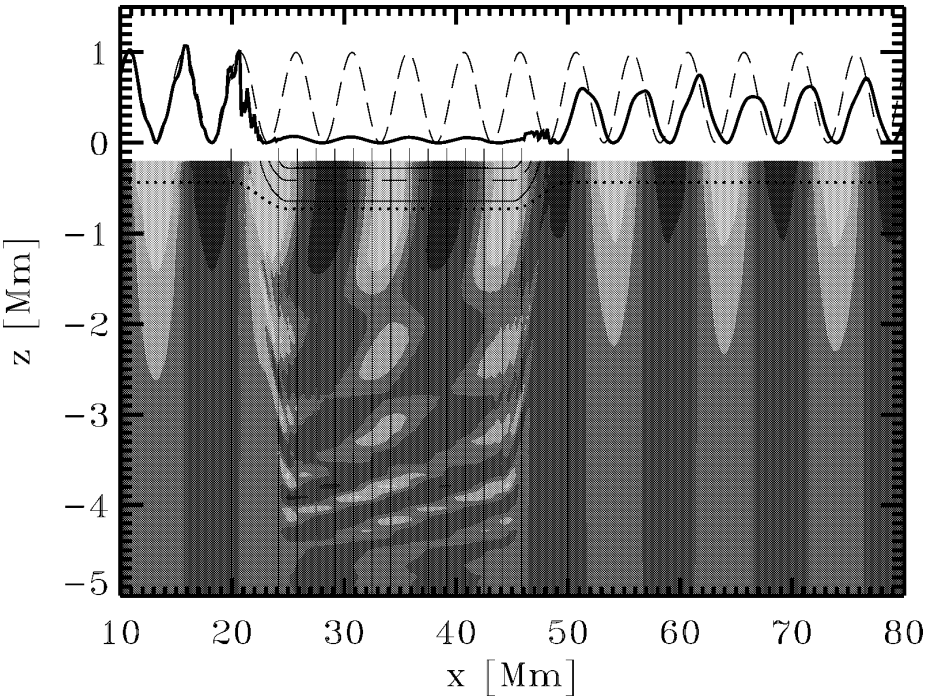

FIG. 1.—Contour plot of the horizontal velocity $u(x, z)$ for an f-mode of frequency $\nu = 2.09$ mHz and degree $l = 437$ incident from the left upon a slab of vertical magnetic field situated between $x = 20$ Mm and $x = 50$ Mm (*bottom*). The thin vertical lines represent the equilibrium magnetic field, with equal flux between successive field lines. The dashed line near the top of the slab shows the location of the $a = c$ surface (a and c are the Alfvén and sound speeds, respectively), and the neighboring solid lines enclose the region where $10^{-1/2} < a^2/c^2 < 10^{1/2}$. The dotted line that runs just below these three curves marks the location of the $T = 5775$ K isotherm, which corresponds to the minimum temperature in the nonmagnetic enhanced polytrope. The solid line plot (*top*) shows the square of the vertical velocity w^2 along the $T = 5775$ K isotherm. The dashed curve indicates w^2 along the same isotherm if the field concentration is not present. Note the disparity in the x and z scales in this figure.

CALLY & BOGDAN (see 486, L68)

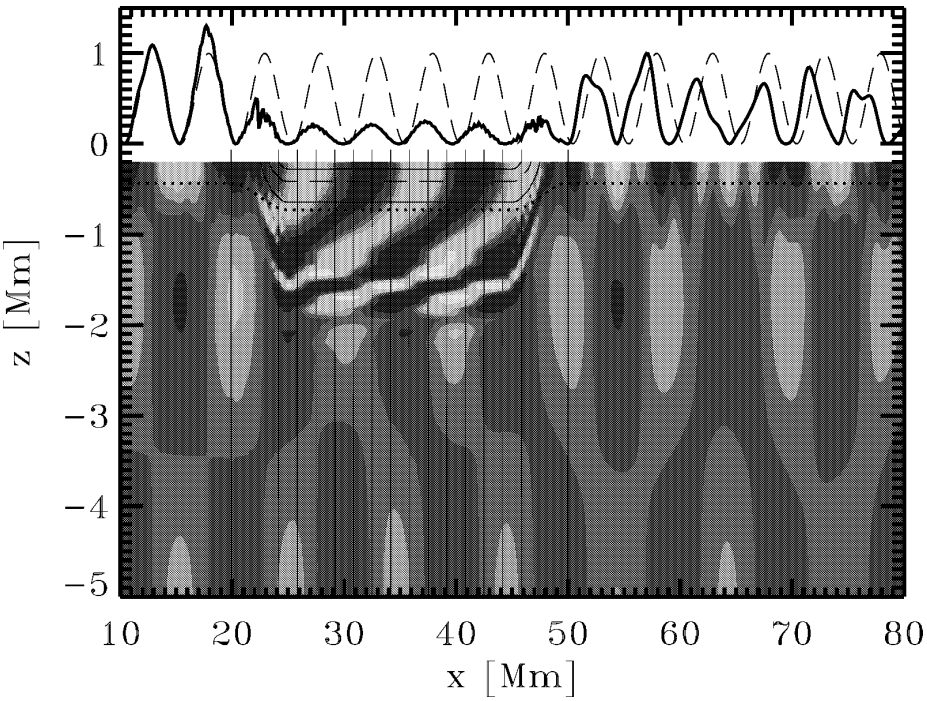

FIG. 2.—The same as Fig. 1, except for an incident p_2-mode of frequency $\nu = 4.08$ mHz and degree $l = 437$. Note the very apparent rightward propagating f-modes of the same frequency but shorter wavelength and correspondingly lower phase speed to the right of the slab, indicating substantial mode-mixing. Although the s-modes propagating down the field lines appear to die out at about $z = -2$ Mm in this figure, this is an illusion due to the greater intensity of the p-mode at these depths. In fact, the s-modes are apparent in contour plots of b_x down to at least $z = -10$ Mm. Similar comments apply to Figs. 3 and 4. The lower turning point for the p_2-mode in the enhanced polytrope is situated below the region displayed in this plot.

CALLY & BOGDAN (see 486, L68)

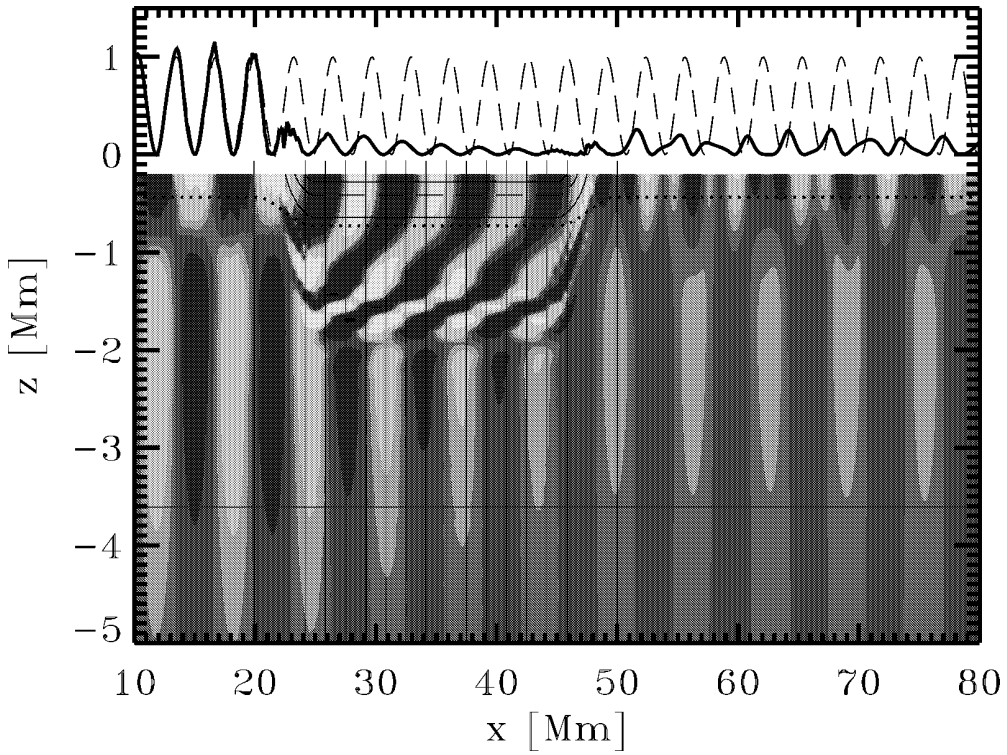

FIG. 3.—The same as Fig. 1, except for an incident p_1-mode of frequency $\nu = 4.08$ mHz and degree $l = 674$. Mode-mixing into f-modes is again apparent. The thin solid horizontal line marks the lower turning point of this mode in the enhanced polytrope where the horizontal phase speed matches the local sound speed.

CALLY & BOGDAN (see 486, L68)

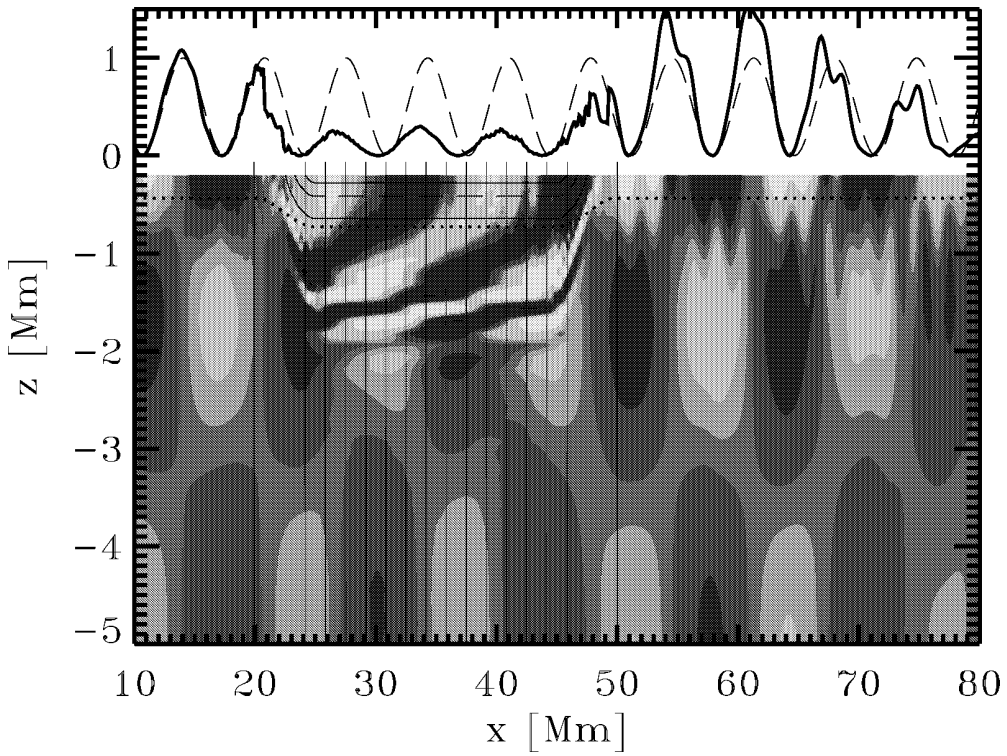

FIG. 4.—The same as Fig. 1, except for an incident p_3-mode of frequency $\nu = 4.08$ mHz and degree $l = 323$. Mode-mixing into f-modes is again apparent and indeed appears responsible for the *increased* vertical velocity to the right of the slab wherever p_3 and f modes reinforce. The lower turning point for the p_3-mode in the enhanced polytrope is situated well below the region displayed in this plot.

CALLY & BOGDAN (see 486, L68)